PERGAMON

International Journal of Solids and Structures 37 (2000) 4859–4869

INTERNATIONAL JOURNAL OF SOLIDS and STRUCTURES

www.elsevier.com/locate/ijsolstr

Analysis of stress and electric fields in a rectangular piezoelectric body with a center crack under anti-plane shear loading

Soon Man Kwon, Kang Yong Lee*

Department of Mechanical Engineering, Yonsei University, Seoul 120-749, South Korea

Received 29 March 1999; in revised form 15 June 1999

Abstract

The singular stress and electric fields in a rectangular piezoelectric ceramic body containing a Griffith center crack under anti-plane shear loading are obtained by the theory of linear piezoelectricity. Fourier transforms and Fourier sine series are used to reduce the problem to a pair of dual integral equations, which is expressed to a Fredholm integral equation of the second kind. Numerical values on the stress intensity factor and the energy release rate are obtained to show the influence of the electric field.

Keywords: Piezoelectric materials; Anti-plane shear; Fredholm integral equation; Intensity factors; Energy release rate

1. Introduction

Piezoelectric ceramic materials are used widely owing to their high piezoelectric performance, but the inherent weakness of piezoelectric ceramics is its brittleness. Severe mechanical stress occurs in use. The stress concentrations under mechanical and electric loads may cause crack initiation and propagation. To improve the performance and to predict the reliable service lifetime of ceramic piezoelectric components, it is necessary to analyze theoretically the damage and fracture processes taking place in piezoelectric materials with consideration of the coupled effects of mechanics and electrics. The study in fracture mechanics of piezoelectric ceramics has been paid more attention to in recent years. Deeg (1980) and Pak (1990) addressed the plane and anti-plane fracture problems of an infinite piezoelectric body and obtained the closed form solutions of stress field and electric displacement near the crack tip. With the aid of the three-dimensional eigenfunction expansion method, Sosa and Pak (1990)

* Corresponding author.
E-mail address: fracture@yonsei.ac.kr (K.Y. Lee).

0020-7683/00/$ - see front matter
PII: S0020-7683(99)00186-9

investigated the infinite body with the straight crack front located along the transversely isotropic axis of symmetry and they discussed the influence of electric fields to the stress field near the crack tip. Sosa (1991) suggested a general method of solving plane problems of piezoelectric media with defects. Recently, Park and Sun (1995) obtained the closed form solutions for all three modes of fracture for an infinite piezoelectric medium containing a center crack subjected to a combined mechanical and electric loading. Pak (1992) suggested the closed form solution for an infinite piezoelectric body under anti-plane loading by employing a complex variable approach. Also Shindo et al. (1996, 1997) obtained the solution of the infinite strip parallel or perpendicular to the crack under anti-plane loading using integral transform method.

In this paper, we apply the theory of linear piezoelectricity to the electroelastic problem of a center crack in a rectangular piezoelectric ceramics under anti-plane shear loading. Fourier cosine transforms and Fourier sine series are used to obtain a pair of dual integral equations, which is then expressed into a Fredholm integral equation of the second kind. Numerical results for the stress intensity factor and the energy release rate are shown graphically for various piezoelectric ceramics.

2. Problem statements and method of solution

Consider a piezoelectric body in the form of a rectangular sheet containing a center crack subjected to mechanical and electrical loads as shown in Fig. 1. We will consider four possible cases of boundary conditions at the edges of the rectangular sheet. The piezoelectric material with the poling axis z occupies the region $(-b \le x \le b,\ -h \le y \le h)$, and is thick enough in the z-direction to allow a state of anti-plane shear. The crack is located at the center $(-a \le x \le a,\ y = 0)$. Because of the assumed symmetry in geometry and loading, it is sufficient to consider the problem for $0 \le x \le b,\ 0 \le y \le h$ only.

The piezoelectric boundary value problem is simplified considerably if we consider only the out-of-plane displacement and the in-plane electric fields in the forms

$$u_x = u_y = 0, \quad u_z = w(x, y), \quad E_x = E_x(x, y), \quad E_y = E_y(x, y), \quad E_z = 0. \tag{1}$$

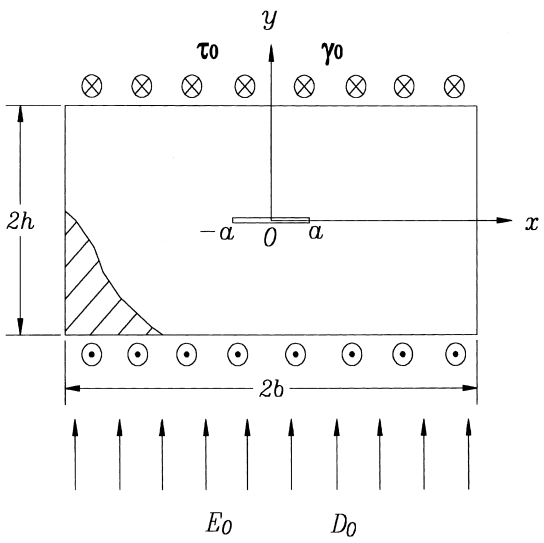

Fig. 1. Rectangular piezoelectric body with a center crack subjected to in-plane electric loads and anti-plane mechanical loads.

where u_i and E_i $(i = x, y, z)$ are the displacement and electric field vectors, respectively. In this case the constitutive relations become

$$\tau_{xz} = c_{44}\frac{\partial w}{\partial x} + e_{15}\frac{\partial \phi}{\partial x}, \qquad \tau_{yz} = c_{44}\frac{\partial w}{\partial y} + e_{15}\frac{\partial \phi}{\partial y}, \tag{2}$$

$$D_x = e_{15}\frac{\partial w}{\partial x} - d_{11}\frac{\partial \phi}{\partial x}, \qquad D_y = e_{15}\frac{\partial w}{\partial y} - d_{11}\frac{\partial \phi}{\partial y}, \tag{3}$$

where τ_{kz}, D_k, $(k = x, y)$, c_{44}, d_{11}, e_{15} and ϕ are the stress tensor, the electric displacement vector, the elastic modulus measured in a constant electric field, the dielectric permittivity measured at a constant strain, the piezoelectric constant and the electric potential, respectively. The governing equations are simplified to

$$c_{44}\nabla^2 w + e_{15}\nabla^2 \phi = 0,$$

$$e_{15}\nabla^2 w - d_{11}\nabla^2 \phi = 0. \tag{4}$$

where $\nabla^2 = \partial^2/\partial x^2 + \partial^2/\partial y^2$ is the two-dimensional Laplacian operator in the variables x and y.

The boundary conditions are written as

$$\begin{aligned} &\tau_{yz}(x, 0) = 0, \quad (0 \le x < a), \\ &w(x, 0) = 0, \quad (a < x \le b), \end{aligned} \tag{5}$$

$$\begin{aligned} &\tau_{xz}(b, y) = 0, \quad (0 \le y \le h), \\ &D_x(b, y) = 0, \quad (0 \le y \le h), \end{aligned} \tag{6}$$

$$\begin{aligned} &E_x(x, 0) = E_x^c(x, 0), \quad (0 \le x < a), \\ &\phi(x, 0) = 0, \quad (a < x \le b), \end{aligned} \tag{7}$$

where the superscript c represents the electric quantities in the crack. There may be the four cases of combined electric and mechanical loadings as follows:

$$\text{Case 1:} \quad \tau_{yz}(x, h) = \tau_0 \quad \text{and} \quad D_y(x, h) = D_0, \tag{8}$$

$$\text{Case 2:} \quad \gamma_{yz}(x, h) = \gamma_0 \quad \text{and} \quad E_y(x, h) = E_0, \tag{9}$$

$$\text{Case 3:} \quad \tau_{yz}(x, h) = \tau_0 \quad \text{and} \quad E_y(x, h) = E_0, \tag{10}$$

$$\text{Case 4:} \quad \gamma_{yz}(x, h) = \gamma_0 \quad \text{and} \quad D_y(x, h) = D_0, \tag{11}$$

where τ_0, D_0, γ_0 and E_0 are uniform applied shear traction, uniform applied electric displacement, uniform applied shear strain and uniform applied electric field, respectively. The solutions of the displacement component $w(x, y)$ and the electric potential $\phi(x, y)$ for Eq. (4) are given in terms of the following Fourier cosine transform and Fourier sine series (Chang, 1985):

$$w(x, y) = \frac{2}{\pi}\int_0^\infty A_1(s)\frac{\cosh[s(h - y)]}{\cosh(sh)}\cos(sx)\,\mathrm{d}s + \sum_{n=0}^{\infty} B_1(n)\cosh(\beta_n x/h)\sin(\beta_n y/h) + a_0 y, \tag{12}$$

$$\phi(x,y)=\frac{2}{\pi}\int_0^\infty A_2(s)\frac{\cosh\left[s(h-y)\right]}{\cosh(sh)}\cos(sx)\,\mathrm{d}s+\sum_{n=0}^{\infty}B_2(n)\cosh\left(\beta_n x/h\right)\sin\left(\beta_n y/h\right)-b_0 y, \tag{13}$$

where $A_i(s)$, $B_i(n)$ $(i=1,2)$ are the unknowns to be solved, a_0 and b_0 are real constants which are determined from the edge loading conditions, and $\beta_n=(2n+1)\pi/2$.

The corresponding stress and electric displacement components may be obtained with the aid of Eqs. (2) and (3):

$$\begin{aligned}\tau_{xz}(x,y)=&-\frac{2}{\pi}\int_0^\infty s\left[c_{44}A_1(s)+e_{15}A_2(s)\right]\frac{\cosh\left[s(h-y)\right]}{\cosh(sh)}\sin(sx)\,\mathrm{d}s\\&+\sum_{n=0}^{\infty}\frac{\beta_n}{h}\left[c_{44}B_1(n)+e_{15}B_2(n)\right]\sinh\left(\beta_n x/h\right)\sin\left(\beta_n y/h\right),\end{aligned} \tag{14a}$$

$$\begin{aligned}\tau_{yz}(x,y)=&-\frac{2}{\pi}\int_0^\infty s\left[c_{44}A_1(s)+e_{15}A_2(s)\right]\frac{\sinh\left[s(h-y)\right]}{\cosh(sh)}\cos(sx)\,\mathrm{d}s\\&+\sum_{n=0}^{\infty}\frac{\beta_n}{h}\left[c_{44}B_1(n)+e_{15}B_2(n)\right]\cosh\left(\beta_n x/h\right)\cos\left(\beta_n y/h\right)+c_0,\end{aligned} \tag{14b}$$

$$\begin{aligned}D_x(x,y)=&-\frac{2}{\pi}\int_0^\infty s\left[e_{15}A_1(s)-d_{11}A_2(s)\right]\frac{\cosh\left[s(h-y)\right]}{\cosh(sh)}\sin(sx)\,\mathrm{d}s\\&+\sum_{n=0}^{\infty}\frac{\beta_n}{h}\left[e_{15}B_1(n)-d_{11}B_2(n)\right]\sinh\left(\beta_n x/h\right)\sin\left(\beta_n y/h\right),\end{aligned} \tag{15a}$$

$$\begin{aligned}D_y(x,y)=&-\frac{2}{\pi}\int_0^\infty s\left[e_{15}A_1(s)-d_{11}A_2(s)\right]\frac{\sinh\left[s(h-y)\right]}{\cosh(sh)}\cos(sx)\,\mathrm{d}s\\&+\sum_{n=0}^{\infty}\frac{\beta_n}{h}\left[e_{15}B_1(n)-d_{11}B_2(n)\right]\cosh\left(\beta_n x/h\right)\cos\left(\beta_n y/h\right)+d_0,\end{aligned} \tag{15b}$$

where

$$c_0=c_{44}a_0-e_{15}b_0,\qquad d_0=e_{15}a_0+d_{11}b_0. \tag{16}$$

By applying the edge loading conditions at $y=h$, the constants a_0 and b_0 are evaluated as follows:

$$\text{Case 1:}\quad a_0=\frac{d_{11}\tau_0+e_{15}D_0}{c_{44}d_{11}+e_{15}^2}=\frac{\tau_0}{\mu_e}+\frac{D_0}{e_e},\qquad b_0=\frac{c_{44}D_0-e_{15}\tau_0}{c_{44}d_{11}+e_{15}^2}=\frac{D_0}{d_e}-\frac{\tau_0}{e_e}, \tag{17}$$

$$\text{Case 2:}\quad a_0=\gamma_0,\qquad b_0=E_0, \tag{18}$$

$$\text{Case 3:}\quad a_0=\frac{\tau_0+e_{15}E_0}{c_{44}},\qquad b_0=E_0, \tag{19}$$

$$\text{Case 4:}\quad a_0=\gamma_0,\qquad b_0=\frac{D_0-e_{15}\gamma_0}{d_{11}}, \tag{20}$$

where d_e, μ_e and e_e are the effective dielectric permittivity, effective shear modulus and effective piezoelectric constant of the material, respectively, which are given as follows (Zhang and Hack, 1992; Zhang and Tong, 1996),

$$d_e = d_{11} + e_{15}^2/c_{44}, \quad \mu_e = c_{44} + e_{15}^2/d_{11}, \quad e_e = e_{15} + c_{44}d_{11}/e_{15}. \tag{21}$$

Introducing Eqs. (14a) and (15a) into Eq. (6), we have the following relations,

$$B_k(n) = \frac{4}{\pi h \cdot \sinh(\beta_n b/h)} \int_0^\infty \frac{s}{s^2 + (\beta_n/h)^2} A_k(s)\sin(sb)\,\mathrm{d}s, \quad (k = 1, 2). \tag{22}$$

Substituting Eqs. (12) and (14b) into Eq. (5) and using the facts that the unknowns $A_2(s) = B_2(n) = 0$ which are obtained from Eq. (7), a pair of dual integral equations is obtained,

$$\begin{aligned} &\int_0^\infty sA_1(s)\tanh(sh)\cos(sx)\,\mathrm{d}s - \frac{\pi}{2}\sum_{n=0}^{\infty}\frac{\beta_n}{h}B_1(n)\cosh\left(\frac{\beta_n x}{h}\right) = \frac{\pi}{2}\frac{c_0}{c_{44}}, \quad 0 \le x < a, \\ &\int_0^\infty A_1(s)\cos(sx)\,\mathrm{d}s = 0, \qquad\qquad a < x \le b. \end{aligned} \tag{23}$$

Let

$$A_1(s) = \int_0^a \xi \mho(\xi) J_0(s\xi)\,\mathrm{d}\xi, \tag{24}$$

where $J_0(s\xi)$ stands for the zero order Bessel function of the first kind.

Inserting Eq. (24) into Eq. (23) and considering Eq. (22), we can find that the auxiliary function $\mho(\xi)$ is given by a Fredholm integral equation of the second kind in the form,

$$\mho(\xi) + \int_0^a \mho(\eta)\big[K_1(\xi, \eta) - K_2(\xi, \eta)\big]\,\mathrm{d}\eta = \frac{\pi}{2}\frac{c_0}{c_{44}}, \tag{25}$$

where

$$K_1(\xi, \eta) = \eta \int_0^\infty s\big[\tanh(sh) - 1\big]J_0(s\xi)J_0(s\eta)\,\mathrm{d}s, \tag{26}$$

$$K_2(\xi,\eta) = \eta \sum_{n=0}^{\infty} \frac{\pi(\beta_n/h)\mathrm{e}^{-\beta_n b/h}}{h \cdot \sinh(\beta_n b/h)} I_0(\beta_n \xi/h) I_0(\beta_n \eta/h), \tag{27}$$

and $I_0(\cdots)$ denotes the modified zero order Bessel function of the first kind.

We introduce the following dimensionless variables and functions for numerical analysis;

$$\begin{aligned} &s = S/a, \ \xi = a\Xi, \ \eta = aH, \ \tilde{h} = a/h, \ \tilde{b} = a/b, \\ &\mho(\xi) = \frac{\pi}{2}\frac{c_0}{c_{44}}\frac{\Omega(\Xi)}{\sqrt{\Xi}}, \quad \mho(\eta) = \frac{\pi}{2}\frac{c_0}{c_{44}}\frac{\Omega(H)}{\sqrt{H}}. \end{aligned} \tag{28}$$

Substituting Eq. (28) into Eq. (25), we can obtain a Fredholm integral equation of the second kind in the form,

$$\Omega(\Xi) + \int_0^1 \Omega(H)\big[L_1(\Xi, H) - L_2(\Xi, H)\big]\,\mathrm{d}H = \sqrt{\Xi}, \tag{29}$$

where

$$L_1(\Xi,H) = \sqrt{\Xi H}\int_0^\infty S\left[\tanh\left(S/\tilde{h}\right) - 1\right]J_0(S\Xi)J_0(SH)\,\mathrm{d}s, \tag{30}$$

$$L_2(\Xi, H) = \sqrt{\Xi H}\sum_{n=0}^{\infty}\frac{\pi\beta_n\tilde{h}^2 \mathrm{e}^{-\beta_n\tilde{h}/\tilde{b}}}{\sinh\left(\beta_n\tilde{h}/\tilde{b}\right)}I_0\left(\beta_n\tilde{h}\Xi\right)I_0\left(\beta_n\tilde{h}H\right)$$

$$= \sqrt{\Xi H}\sum_{n=0}^{\infty}\pi\beta_n\tilde{h}^2\left[\coth\left(\beta_n\tilde{h}/\tilde{b}\right) - 1\right]I_0\left(\beta_n\tilde{h}\Xi\right)I_0\left(\beta_n\tilde{h}H\right). \tag{31}$$

In view of practical applications, $\Omega(1)$ values may be approximately expressed by convenient polynomial form using the iterative scheme, that is

$$\Omega(1) = 1 + 0.2056\,\tilde{h}^2 - 0.0909\,\tilde{h}^4 + \sum_{n=0}^{\infty}\frac{\mathrm{e}^{-\beta_n\tilde{h}/\tilde{b}}}{\sinh\left(\beta_n\tilde{h}/\tilde{b}\right)}\left(2.4674\,\tilde{h}^3 n + 1.0146\,\tilde{h}^4 n + 2.2930\tilde{h}^4 n^3\right)$$

$$+ \sum_{m=0}^{\infty}\sum_{n=0}^{\infty}\frac{\mathrm{e}^{-(\beta_m+\beta_n)\tilde{h}/\tilde{b}}}{\sinh\left(\beta_m\tilde{h}/\tilde{b}\right)\sinh\left(\beta_n\tilde{h}/\tilde{b}\right)}6.088\,\tilde{h}^4 mn + O\left(\tilde{h}^6\right). \tag{32}$$

3. Intensity factors and energy release rate

The mode III stress intensity factor, K_{III} is defined and determined in the form,

$$K_{\mathrm{III}} \equiv \lim_{x\to a^+}\sqrt{2\pi(x-a)}\tau_{yz}(x,0) = c_0\sqrt{\pi a}\Omega(1). \tag{33}$$

Extending the traditional concept of stress intensity factors to other field variables, we have

$$\begin{aligned}
\gamma_{xz} &= -\frac{K^\gamma}{\sqrt{2\pi r}}\sin\left(\frac{\theta}{2}\right), \quad \gamma_{yz} = \frac{K^\gamma}{\sqrt{2\pi r}}\cos\left(\frac{\theta}{2}\right),\\
E_x &= -\frac{K^E}{\sqrt{2\pi r}}\sin\left(\frac{\theta}{2}\right), \quad E_\gamma = \frac{K^E}{\sqrt{2\pi r}}\cos\left(\frac{\theta}{2}\right),\\
\tau_{xz} &= -\frac{K^\sigma}{\sqrt{2\pi r}}\sin\left(\frac{\theta}{2}\right), \quad \tau_{yz} = \frac{K^\sigma}{\sqrt{2\pi r}}\cos\left(\frac{\theta}{2}\right),\\
D_x &= -\frac{K^D}{\sqrt{2\pi r}}\sin\left(\frac{\theta}{2}\right), \quad D_y = \frac{K^D}{\sqrt{2\pi r}}\cos\left(\frac{\theta}{2}\right),
\end{aligned} \tag{34}$$

where K^γ is the strain intensity factor, K^E is the electric field intensity factor, K^σ is the stress intensity factor and K^D is the electric displacement intensity factor. These field intensity factors are defined as

$$K^\gamma \equiv \lim_{x\to a^+}\sqrt{2\pi(x-a)}\gamma_{yz}(x,0) = \frac{K_{\mathrm{III}}}{c_{44}} = \frac{c_0}{c_{44}}\sqrt{\pi a}\Omega(1),$$

$$K^E \equiv \lim_{x\to a^+}\sqrt{2\pi(x-a)}E_y(x,0) = 0,$$

$$K^{\sigma} \equiv \lim_{x \to a^{+}} \sqrt{2\pi(x-a)}\tau_{yz}(x,0) = K_{\mathrm{III}} = c_0\sqrt{\pi a}\Omega(1),$$

$$K^{D} \equiv \lim_{x \to a^{+}} \sqrt{2\pi(x-a)}D_{y}(x,0) = \frac{e_{15}}{c_{44}}K_{\mathrm{III}} = \frac{e_{15}c_0}{c_{44}}\sqrt{\pi a}\Omega(1). \tag{35}$$

Evaluating the energy release rate G for the anti-plane case obtained by Pak (1990) on vanishingly small contour at a crack tip, we obtain

$$G = \frac{K^{\gamma}K^{\sigma}}{2} = \frac{K_{\mathrm{III}}^{2}}{2c_{44}} = \frac{\pi a}{2c_{44}}c_0^2\Omega^2(1). \tag{36}$$

Equation (36) shows that the energy release rate are positive, which was well referred to by Gao et al. (1997). The energy release rate is only determined by the applied stress. This is agreed with the results of Zhang and Tong (1996) and Gao et al. (1997). From Eq. (36), we obtain the energy release rates for four possible boundary conditions

$$\text{Case 1:} \quad G = \frac{\pi a}{2c_{44}}\tau_0^2\Omega^2(1), \tag{37}$$

$$\text{Case 2:} \quad G = \frac{\pi a}{2c_{44}}(c_{44}\gamma_0 - e_{15}E_0)^2\Omega^2(1), \tag{38}$$

$$\text{Case 3:} \quad G = \frac{\pi a}{2c_{44}}\tau_0^2\Omega^2(1), \tag{39}$$

$$\text{Case 4:} \quad G = \frac{\pi a}{2c_{44}}\left(\mu_e\gamma_0 - \frac{e_{15}D_0}{d_{11}}\right)^2\Omega^2(1). \tag{40}$$

From Eqs. (37)–(40), it is noted that the energy release rates are dependent on the electric loading only under constant strain loading and independent on it under constant stress loading. These are agreed with Zhang and Tong (1996).

Since $\Omega(1) \to 1$ from Eq. (29) as $b \to \infty$ and $h \to \infty$, the energy release rate G_{∞} for an infinite piezoelectric ceramic can be obtained from Eqs. (37)–(40) as

$$G_{\infty} = \frac{\pi a}{2c_{44}}c_0^2. \tag{41}$$

Equation (41) is also agreed with Zhang and Hack (1992) and Zhang and Tong (1996).

4. Discussions

The solution of an infinite piezoelectric strip containing a central crack parallel to the strip edges ($b \to \infty$ or $\tilde{b} \to 0$) can be derived from Eqs. (29)–(31) by using the result

$$\lim_{\tilde{b} \to 0}\left[\frac{\mathrm{e}^{-\beta_n\tilde{h}/\tilde{b}}}{\sinh\left(\beta_n\tilde{h}/\tilde{b}\right)}\right] = 0. \tag{42}$$

In this case, the function $\Omega(1)$ is governed by

$$\Omega(\Xi) + \int_0^1 \Omega(H)L_1(\Xi, H)\,\mathrm{d}H = \sqrt{\Xi}, \tag{43}$$

because the function $L_2(\Xi, H)$ represented by the Eq. (31) is obviouly vanished, Eq. (43) is the same as the result of Shindo et al. (1997).

Letting $h\to\infty(\tilde{h}\to 0)$ in Eqs. (29)–(31), and considering

$$\lim_{\tilde{h}\to 0}\left[\tanh\left(S/\tilde{h}\right)-1\right]=0, \tag{44}$$

and assuming $\lim_{\tilde{h}\to 0}(\pi\tilde{h}) = \mathrm{d}S$; $\beta\tilde{h}=S$, the solution of a piezoelectric strip with a central crack perpendicular to its edges may be also obtained from Eq. (29) in the forms:

$$\Omega(\Xi)+\int_0^1 \Omega(H)L_3(\Xi,H)\,\mathrm{d}H=\sqrt{\Xi}, \tag{45}$$

where

$$L_3(\Xi,H)=-\sqrt{\Xi H}\int_0^\infty \frac{Se^{-S/\tilde{b}}}{\sinh\left(S/\tilde{b}\right)}I_0(S\Xi)I_0(SH)\,\mathrm{d}S$$

$$=\sqrt{\Xi H}\int_0^\infty S\left[1-\coth\left(S/\tilde{b}\right)\right]I_0(S\Xi)I_0(SH)\,\mathrm{d}S, \tag{46}$$

Eqs. (45) and (46) are also identical to the result of Shindo et al. (1996).

To examine the effect of electromechanical interactions on the stress intensity factor and the energy release rate, Eq. (29) was computed numerically by the use of Gaussian quadrature formulas. We consider PZT-6B, $BaTiO_3$ and PZT-5H ceramics, and the material properties are listed in Table 1.

Figures 2 and 3 display the variation of the normalized stress intensity factor $\tilde{K}_{\mathrm{III}}=K_{\mathrm{III}}/c_0\sqrt{\pi a}$ and energy release rate G/G_∞ against normalized sample lengths $\tilde{h}=a/h$ and $\tilde{b}=a/b$ with fixed $\tilde{b}$ and $\tilde{h}$ values, respectively. From these results, we can find that the normalized stress intensity factor $\tilde{K}_{\mathrm{III}}$ and energy release rate G/G_∞ increase as $\tilde{b}$ and $\tilde{h}$ values increase at fixed $\tilde{h}$ and $\tilde{b}$, respectively. Especially, the effects of normalized sample width $\tilde{b}$ on the stress intensity factor and energy release rate are greater than those of normalized sample height $\tilde{h}$.

Figures 4 and 5 show the variation of the normalized energy release rate G/G_{cr} against E_0 and D_0, respectively. In cases 2 and 4, the minimum normalized energy release rate G/G_{cr} can exist with the variation of electrical load but has always positive values.

Table 1
Material properties of piezoelectric ceramics (Shindo et al., 1997)

Material properties	Symbol	Unit	Piezoceramics		
			PZT-6B	$BaTiO_3$	PZT-5H
Elastic stiffness	c_{44}	$\times 10^{10}$ N/m^2	2.71	4.3	3.53
Piezoelectric constants	e_{15}	C/m^2	4.6	11.6	17.0
Dielectric permittivity	d_{11}	$\times 10^{-10}$ F/m	36.0	112.0	151.0
Critical energy release rate	G_{cr}	J/m^2	5.0	4.0	5.0

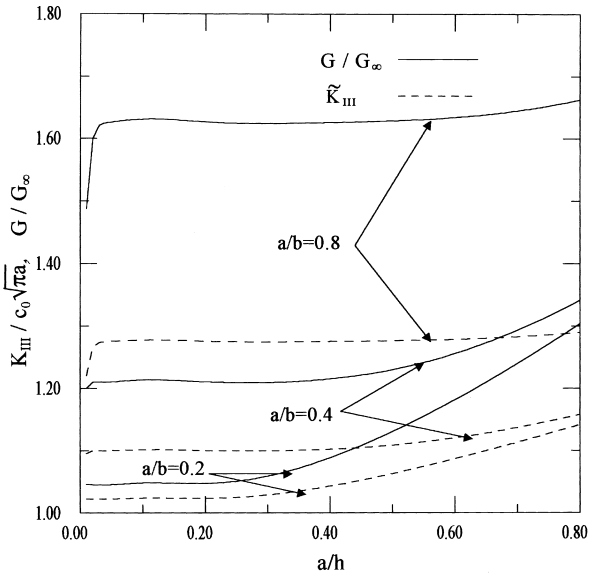

Fig. 2. Normalized stress intensity factor $\tilde{K}_{III}$ and energy release rate G/G_∞ vs. normalized sample height $\tilde{h}$.

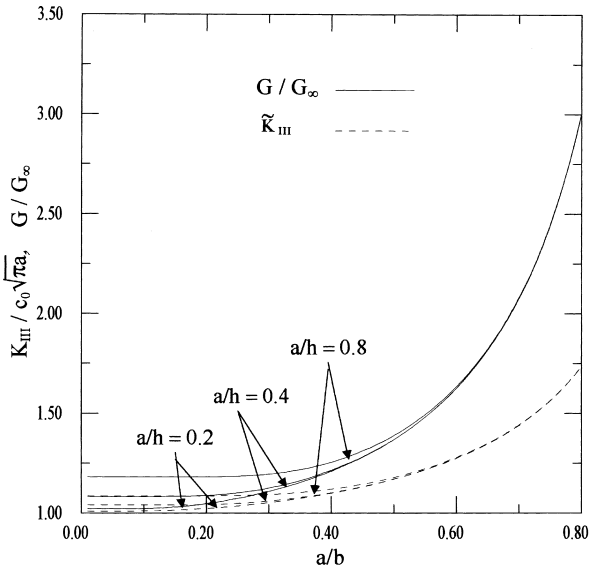

Fig. 3. Normalized stress intensity factor $\tilde{K}_{III}$ and energy release rate G/G_∞ vs. normalized sample width $\tilde{b}$.

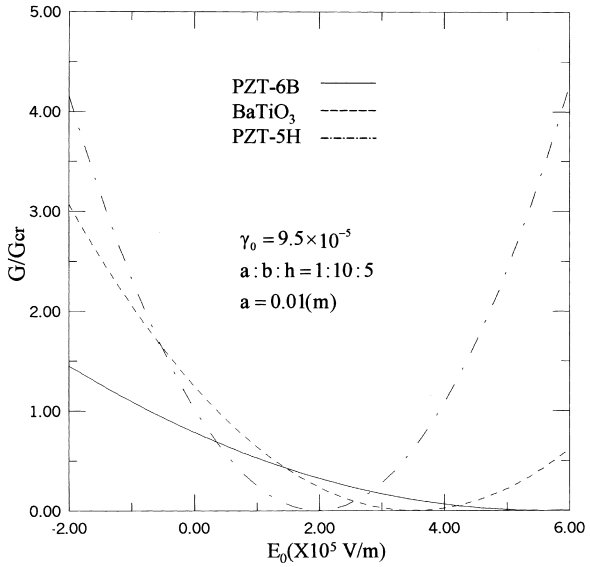

Fig. 4. Normalized energy release rate of piezoelectric ceramics (Case 2).

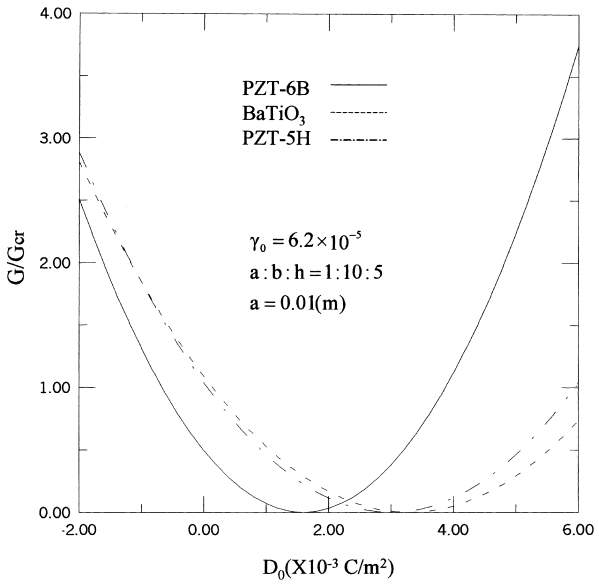

Fig. 5. Normalized energy release rate of piezoelectric ceramics (Case 4).

5. Conclusions

The electroelastic problem of a central crack in a rectangular transversely isotropic piezoelectric ceramic under anti-plane shear was analyzed by the integral transform approach. The traditional concept of linear elastic fracture mechanics is extended to include the piezoelectric effects. The results are expressed in terms of the stress intensity factor and the energy release rate. The following conclusions are obtained:

1. The energy release rate are dependent on the electric loading only under constant strain loading and independent of it under constant stress loading.
2. The normalized stress intensity factor and the normalized energy release rate increase when the normalized sample lengths $\tilde{h}$ and $\tilde{b}$ are increased.
3. The effects of normalized sample width $\tilde{b}$ on the stress intensity factor and energy release rate are greater than those of normalized sample height $\tilde{h}$.
4. In constant strain loadings, the minimum normalized energy release rate G/G_{cr} can exist with the variation of electrical load but has always positive values.

Acknowledgements

The authors are grateful for the support provided by a grant from the Korea Science and Engineering Foundation (KOSEF) and Safety and Structural Integrity Research Center at the Sungkyunkwan University.

References

Chang, S.S., 1985. The solution of a rectangular orthotropic sheet with a central crack under anti-plane shear. Engineering Fracture Mechanics 22, 253–261.

Deeg, W.F., 1980. The analysis of dislocation, crack, and inclusion problems in piezoelectric solids. Ph.D. Thesis, Stanford University, Stanford, CA.

Gao, H., Zhang, T.Y., Tong, P., 1997. Local and global energy release rates for an electrically yielded crack in a piezoelectric ceramic. Journal of the Mechanics and Physics of Solids 45, 491–510.

Pak, Y.E., 1990. Crack extension force in a piezoelectric materials. ASME Journal of Applied Mechanics 57, 647–653.

Pak, Y.E., 1992. Linear electroelastic fracture mechanics of piezoelectric materials. International Journal of Fracture 54, 79–100.

Park, S.B., Sun, C.T., 1995. Effect of electric field on fracture of piezoelectric ceramics. International Journal of Fracture 70, 203–216.

Shindo, Y., Narita, F., Tanaka, K., 1996. Electroelastic intensification near anti-plane shear crack in orthotropic piezoelectric ceramic strip. Theoretical and Applied Fracture Mechanics 25, 65–71.

Shindo, Y., Tanaka, K., Narita, F., 1997. Singular stress and electric fields of a piezoelectric ceramic strip with a finite crack under longitudinal shear. Acta Mechanica 120, 31–45.

Sosa, H.A., Pak, Y.E., 1990. Three-dimensional eigenfunction analysis of a crack in a piezoelectric material. International Journal of Solids and Structures 26, 1–15.

Sosa, H.A., 1991. Plane problems in piezoelectric media with defects. International Journal of Solids and Structures 28, 491–505.

Zhang, T.Y., Hack, J.E., 1992. Mode-III cracks in piezoelectric materials. Journal of Applied Physics 71, 5865–5870.

Zhang, T.Y., Tong, P., 1996. Fracture mechanics for a mode III crack in a piezoelectric material. International Journal of Solids and Structures 33, 343–359.